Oral bioaccessibility of metal(loid)s in dust materials from mining areas of northern Namibia

Vojtěch Ettler[a,*], Markéta Cihlová[a], Alice Jarošíková[a], Martin Mihaljevič[a], Petr Drahota[a], Bohdan Kříbek[b], Aleš Vaněk[c], Vít Penížek[c], Ondra Sracek[d], Mariana Klementová[e], Zbyněk Engel[f], Fred Kamona[g], Ben Mapani[g]

[a] Institute of Geochemistry, Mineralogy and Mineral Resources, Faculty of Science, Charles University, Albertov 6, 128 43 Prague 2, Czech Republic
[b] Czech Geological Survey, Geologická 6, 152 00 Prague 5, Czech Republic
[c] Department of Soil Science and Soil Protection, Faculty of Agrobiology, Food and Natural Resources, Czech University of Life Sciences Prague, Kamýcká 129, 165 21 Prague 6, Czech Republic
[d] Department of Geology, Faculty of Science, Palacký University in Olomouc, 17. listopadu 12, 771 46 Olomouc, Czech Republic
[e] Institute of Inorganic Chemistry of the Czech Academy of Sciences, Husinec-Řež 1001, 250 68 Řež, Czech Republic
[f] Department of Physical Geography and Geoecology, Faculty of Science, Charles University, Albertov 6, 128 43 Prague 2, Czech Republic
[g] Department of Geology, Faculty of Science, University of Namibia, Private Bag 13301, Windhoek, Namibia

ARTICLE INFO

ABSTRACT

Ore mining and processing in semi-arid areas is responsible for the generation of metal(loid)-containing dust, which is easily transported by wind to the surrounding environment. To assess the human exposure to dust-derived metal(loid)s (As, Cd, Cu, Pb, Sb, Zn), as well as the potential risks related to incidental dust ingestion, we studied mine tailing dust (n = 8), slag dust (n = 5) and smelter dust (n = 4) from old mining and smelting sites in northern Namibia (Kombat, Berg Aukas, Tsumeb). *In vitro* bioaccessibility testing using extraction in simulated gastric fluid (SGF) was combined with determination of grain-size distributions, chemical and mineralogical characterizations and leaching tests conducted on original dust samples and separated PM_{10} fractions. The bulk and bioaccessible concentrations of the metal(loid)s were ranked as follows: mine tailing dusts < slag dusts ≪ smelter dusts. Extremely high As and Pb bioaccessibilities in the smelter dusts were caused by the presence of highly soluble phases such as arsenolite (As_2O_3) and various metal-arsenates unstable under the acidic conditions of SGF. The exposure estimates calculated for an adult person of 70 kg at a dust ingestion rate of 50 mg/day indicated that As, Pb (and also Cd to a lesser extent) grossly exceeded tolerable daily intake limits for these contaminants in the case of slag and smelter dusts. The high risk for smelter dusts has been ac-knowledged, and the safety measures currently adopted by the smelter operator in Tsumeb are necessary to reduce the staff's exposure to contaminated dust. The exposure risk for the local population is only important at the unfenced disposal sites at Berg Aukas, where the PM_{10} exhibited high levels of bioaccessible Pb.

1. Introduction

The health effects related to dusts that can be inhaled or ingested are a well known phenomenon (Csavina et al., 2012; Morman and Plumlee, 2013; Kim et al., 2015). In particular, the mining and ore processing industries are responsible for generation of large amounts of metal(loid)-rich fine dust particles, which become the sources for air and soil pollution (Ettler, 2016; Ettler et al., 2016), adhere to the surfaces of plants (Kříbek et al., 2016, 2018) and/or cause direct health problems in local populations (Plumlee and Morman, 2011; Martin et al., 2014). The risk of dust generation and transport by wind is especially high in arid or semi-arid areas, where the total respirable aerosols (PM_{10}; *i.e.*, particulate matter of grain sizes equal to 10 μm or less) significantly exceed permissible levels as defined by environmental agencies and health organizations (US EPA, WHO) (Ghorbel et al., 2010; Csavina et al., 2012; Thomas et al., 2018). For example, Ojelede et al. (2012) reported that the PM_{10} concentration was > 2000 μg/m^3 at higher wind speeds in the vicinity of a mine tailing site in South Africa; this value far exceeds the 24-h limit value of 150 μg/m^3 stipulated by US EPA.

Apart from the consumption of contaminated water and food, the incidental ingestion and/or inhalation of dust and soil particles

---

represent the key pathways for human exposure to inorganic contaminants (Banza et al., 2009; Swartjes and Cornelis, 2011; Cheyns et al., 2014; Křibek et al., 2014; Zhao et al., 2018). Prior large-scale biomonitoring studies dealing with human exposures to metal(loid)s have traditionally been based on the analysis of contaminants in the blood (Yabe et al., 2015; Bose-O'Reilly et al., 2018), urine (Banza et al., 2009; Cheyns et al., 2014; Yabe et al., 2018), feces (Yabe et al., 2018) or head hair (Boisa et al., 2013). However, these approaches are generally very expensive, they need the approval of health organizations, research institutions or ministries ethics committees, research institutions or ministries of health organizations and samples of the biomarkers are susceptible to contamination.

To overcome these difficulties, numerous *in vitro* bioaccessibility methods have been developed and tested/validated by comparison with *in vivo* tests (generally using pig or mouse models) to evaluate the risks related to incidental dust and/or soil ingestion (*e.g.*, USEPA, 2007; Denys et al., 2012; Deshommes et al., 2012; Li et al., 2016) or inhalation (Molina et al., 2013; Boisa et al., 2014; Alpofead et al., 2016, 2017; Kastury et al., 2018). These bioaccessibility methods have been used at numerous mining sites to assess the human exposure to contaminants from soils (Harvey et al., 2016; Li et al., 2016), urban indoor and outdoor dust (Reis et al., 2014; Harvey et al., 2016), mine tailings (Meunier et al., 2010; Drahota et al., 2018; Thomas et al., 2018) and smelter-derived materials such as slags and flue dust (Boisa et al., 2013; Ettler et al., 2014; Morrison et al., 2016; Ettler et al., 2018).

However, such investigations are still absent in less-developed countries, especially in sub-Saharan Africa. To remedy this gap, we aimed to determine the oral bioaccessibility of arsenic (As), cadmium (Cd), copper (Cu), lead (Pb), antimony (Sb) and zinc (Zn) in mining- and smelting-derived dusts from the old mining districts in the semi-arid areas of northern Namibia. Given the key importance of solid-phase speciation for contaminant release under variable conditions (Romero et al., 2008; Ghorbel et al., 2010; Boisa et al., 2013; Molina et al., 2013; Ettler et al., 2014, 2018; Entwistle et al., 2017; Thomas et al., 2018), we combined bioaccessible leaching tests with detailed physico-chemical and mineralogical investigations of the dusts to estimate the exposure risks for local populations who live close to these areas and/or are working in the mining/smelting industry.

2. Materials and methods

2.1. Sampling areas

We studied dust samples from three old mining and smelting districts located in the Otavi Mountain Land in northern Namibia (Kombat, Berg Aukas and Tsumeb) (Figs. 1a and S1a).

The Kombat site is a Cu-Pb-Zn-Ag deposit mined for sulfides and sulfosalts hosted in carbonate rocks. The mine was active between *ca.* 1900 and 2008, after which it was closed due to flooding (more details about the geology are given in Frimmel et al., 1996; Mileusnic et al., 2014; and Sracek et al., 2014a). Two large mine tailing dams are located south of this mining town (Figs. 1b and S1a).

Berg Aukas is a Pb-Zn-V mineralization in carbonate rocks that was mined between 1920 and 1978 for oxidized sulfide ore bodies with predominant Pb and Zn sulfides, V-bearing mineral descloisite $[(Pb,Zn)_2(OH)VO_4]$ and willemite (Zn_2SiO_4). Apart from two tailing dams located E of the settlement, there are also residues of a former Zn calciner and related slag deposits found in the SW corner of the settlement (Fig. S1a; details are given in Mapani et al., 2010 and Sracek et al., 2014b). The abandoned mining and smelting grounds at Berg Aukas are not fenced in, and children have often been observed playing in these areas (Fig. 1c).

Tsumeb is a world-famous Pb-Cu-Zn deposit developed in limestone and dolomite rocks and exhibiting a spectacular diversity of minerals. The Tsumeb mine was exploited between 1905 and 1996 for Pb, Cu and Zn ores, also with economic concentrations of Ag, Cd, Ge and As. The

Tsumeb smelter has processed local ores since 1907, but after cessation of mining activities in the area, the Pb smelter was dismantled. Dundee Precious Metals Tsumeb (DMPT) Ltd. is still operating the Cu smelter, which currently processes Cu concentrates imported from abroad (Fig. S1b). Numerous slag and old tailing dams are located in and around the smelter area; by-products, intermediate products and waste smelter dusts are stored within the fenced smelter complex (Figs. 1d, e, f, g and S1a). Details regarding the geology, mining history, and smelting technology can be found elsewhere (Frimmel et al., 1996; Ettler et al., 2009; Mapani et al., 2014; Křibek et al., 2016; Ettler et al., 2016; Jarošíková et al., 2017; Křibek et al., 2018).

The three mining sites are located close to the western limit of the Kalahari Desert, and experience a semi-arid climate with average annual precipitations of 481 mm (Berg Aukas), 546 mm (Kombat) and 550 mm (Tsumeb) (most precipitation falls in the period from December to March; climate-data.org). Due to the semi-arid conditions (average annual temperature of ~10 °C) and strong winds which blow in the region, wind erosion and the subsequent transport of dust particles has been documented at each of the sampling sites (*e.g.*, Fig. 1b, d, e).

2.2. Dust sample collection, processing and characterization

All materials were sampled from the surface of the waste disposal sites, which are exposed to wind erosion. Several random grab samples (depths from 0 to 10 cm) were collected using a plastic shovel to make a composite sample weighing approximately 2 kg. We collected the following set of materials: (i) mine tailing dusts originating from the flotation of milled ore materials and deposited on tailing dams (n = 8), (ii) slag dusts originating from granulation of the slag melt at the time of tapping off the furnace and deposited on the dumps (n = 5) and (iii) smelter dusts originating from other stages of smelting technology and/or flue-gas cleaning and deposited on piles within the smelter complex (n = 4) (Table 1, Fig. S1a, b). The samples were stored in zip-locked polyethylene bags and air-dried upon return from the field.

The original dust samples were sieved to < 2 mm to remove large debris; the obtained bulk samples were subsequently used for the bioaccessibility testing in the simulated gastric fluid (SGF). Moreover, the < 10 μm fraction (PM_{10}) of the dusts was obtained by dry sieving through a SEFAR NITEX 03-10/2 polyamide sieve (SEFAR AG, Switzerland; nominal mesh of 10 μm) to only obtain respirable particles (*i.e.*, those that could potentially enter into lung compartments). It is assumed that only particles < 2.5 or 3 μm can access the deep lung (secondary bronchi, bronchioles, and alveoli) and that larger inhaled particles are cleared from the airways by the mucociliary escalator, swallowed, and transported into the gastrointestinal tract (Carvalho et al., 2011; Morman and Plumlee, 2013; Brown et al., 2013; Alpofead et al., 2017; Kastury et al., 2018). For this reason, the PM_{10} obtained was also used for the bioaccessibility testing using SGF. The grain-size distributions of the original and separated dust samples were measured with a HELOS/KF-MAGIC (Sympatec, Germany) laser diffraction analyzer (Figs. 2 and S2). Between 0.3 and 1.5 g of a sample was dispersed in distilled water and an ultrasonic bath for 30 s. Sodium hexametaphosphate was used *prior to* measurement in order to avoid flocculation of fine particles. The samples were measured using Topmicron (R7) and Standard (R3) optical modules to cover a wide range of grain size (up to 3.5 mm) and to detect minor changes of the grain-size distribution at the fine end of the spectrum (31-channel multi-element detector aligned to the 0.5–175 μm measurement range). The two measurements were then combined and the total grain-size distribution reconstructed using QX 2.0 software (Sympatec, Germany). The grain-size distributions confirmed the efficiency of the PM_{10} separation using dry sieving (Fig. S2d).

An aliquot of each sample was finely ground in an agate mortar (Fritsch Pulverisette, Germany) and was used for the determination of bulk chemical compositions after dissolution in mineral acids (HF-
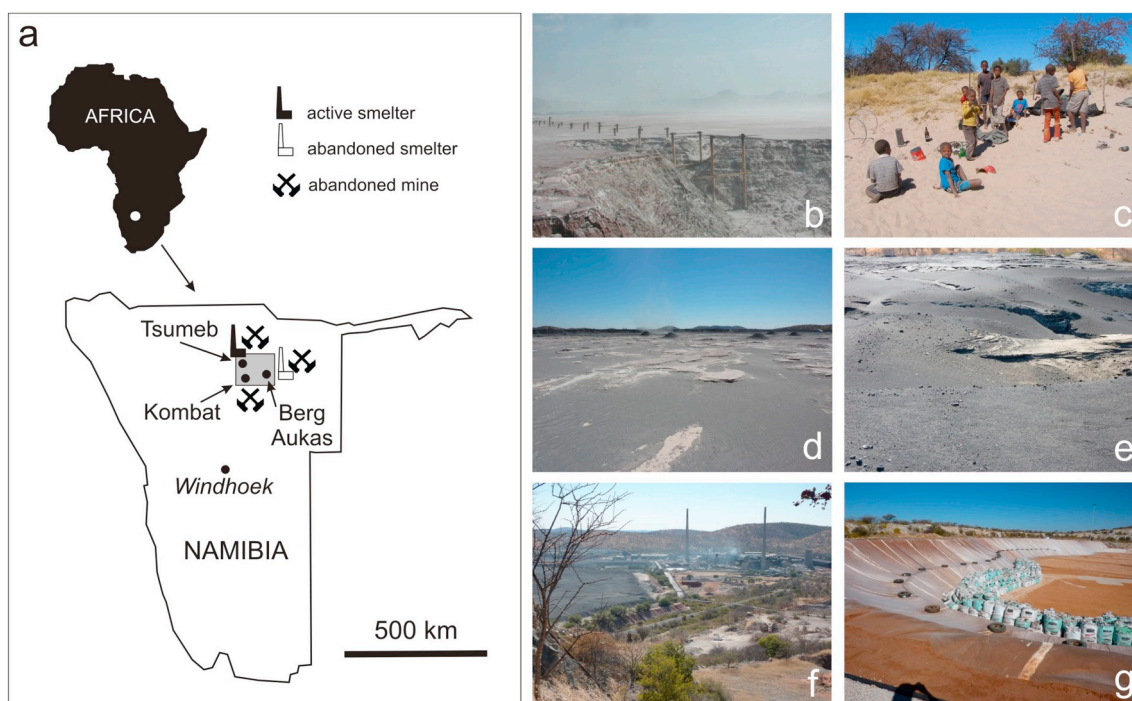
Fig. 1. Map of sampling sites in northern Namibia (a) and photos of the dust dispersion in the studied areas: (b) Windstorm at the Kombat tailing disposal site; (c) Children playing in the dust of the Berg Aukas mine tailing disposal site; (d) Wind erosion of the Tsumeb mine tailing site; (e) Granulated slag disposal at Tsumeb; (f) Dust emissions from the Tsumeb copper smelter and associated mine tailing/slag dumps; (g) Monitored disposal site for the copper smelter flue dust at Tsumeb.

HClO$_4$-HNO$_3$), Lefort *aqua regia* and/or sintering according to Ettler et al. (2009). Concentrations of As, Cd, Cu, Pb, Sb and Zn were determined using either inductively coupled plasma optical emission spectrometry (ICP-OES, ThermoScientific iCAP 6500 radial, UK) or inductively coupled plasma mass spectrometry (ICP-MS, Thermo-Scientific, Xseries^{II}, Germany).

Bulk mineralogy was assessed by X-ray diffraction analysis (XRD) using a PANalytical X'Pert Pro diffractometer (PANalytical, the Netherlands) with a X'Celerator detector, CuKα radiation at 40 kV and 30 mA, over the range 2–80° 2theta, with a step of 0.02° and counting time of 150 s per step. X'Pert HighScore Plus 3.0 software coupled with Crystallography Open Database (COD) (Gražulis et al., 2012) was used for analysis of the XRD patterns.

For scanning electron microscopic (SEM) observations, the dust samples were prepared (i) as polished sections and (ii) as powders mounted onto double-sided conductive tape. The specimens were studied using a TESCAN VEGA3 XM scanning electron microscope (SEM; TESCAN, Czech Republic) equipped with a Quantax 200-X-Flash 5010 energy dispersive X-ray spectrometer (EDS; Bruker, Germany). Polished sections were also examined using a JEOL JXA-8530F electron probe microanalyzer (EPMA; JEOL, Japan) equipped with a field emission gun (FEG) electron source, SEM imaging and quantitative chemical analyses. The transmission electron microscopic (TEM) investigations were carried out on fine-grained smelter dust samples; these specimens were prepared as suspensions in ethanol and pipetted onto carbon-coated Ni grids (SPI, USA). We used a JEOL JEM 3010 microscope (JEOL, Japan), operated at 300 kV (LaB$_6$ cathode, point resolution 1.7 Å), with an attached Oxford Instruments EDS (Oxford Instruments, UK). The images were recorded on a CCD camera with a resolution of 1024 × 1024 pixels, using the Digital Micrograph software package (Gatan, UK). The EDS analyses were acquired and treated with an INCA software package (Oxford Instruments, UK). Selected area electron diffraction patterns (SAED) were evaluated using the Process Diffraction software package (Lábár, 2005).

2.3. Leaching and bioaccessibility tests

The original dust materials were subjected to a batch-leaching test according to European standard EN 12457-2 (EN 12457, 1999), which is used in the EU as a "compliance test" for classifying waste materials for landfilling (EU, 2002). The samples were leached using a L/S (liquid/solid) ratio of 10 L/kg in deionized water at 20 ± 3 °C for 24 h; the duplicated reactors were continuously agitated using a horizontal shaker. After the experiments, the supernatants were filtered to 0.45 μm (Millipore® nitrocellulose membrane filters, USA) and the pH, Eh and specific conductivity values were recorded using Schott multimeters (Schott Gerätte, Germany). The solutions were diluted and analyzed for metal(loid)s by ICP-OES and/or ICP-MS.

The oral bioaccessibility test was performed on the original dusts and PM$_{10}$ according to the US EPA's (2007) protocol in order to investigate the amounts of metal(loid)s that can be extracted in simulated gastric fluid (SGF) (in the literature, this experimental protocol is known as SBRC-G; *i.e.*, gastric phase extraction using the Solubility Bioaccessibility Research Consortium assay). This test was selected due to its simplicity and reliability with *in vivo* tests for Pb (US EPA, 2007; Deshommes et al., 2012) and As (Juhasz et al., 2014a, 2014b); these two elements being major contaminants in our samples (see Table 1). This extraction represents the "worst-case" scenario and the simulated conditions correspond to a fasting human. The sample was extracted in a 0.4 M solution of glycine adjusted to pH 1.5 ± 0.05 by reagent grade HCl (Merck, Germany) at a L/S ratio of 100. The mixture was gently agitated for 1 h at 37 °C in a GFL 3032 incubator (GFL, Germany). All extractions were performed in duplicate and with procedural blanks. According to the experimental protocol, the pH was regularly checked and manually adjusted by drop-addition of HCl in the case of any pH drift caused by the high buffering capacity of the samples (especially those with a high carbonate content) (US EPA, 2007). After the extraction procedures, the solutions were filtered through a 0.45-μm membrane filter, diluted, and analyzed for metal(loid)s by ICP-OES and/or ICP-MS. Subsequently, the bioaccessible concentrations of metal(loid)s were expressed in mg/kg and converted to their percent amount

Table 1
Description, chemical and mineralogical compositions of original dust samples and PM_{10} fractions.

Dust category	Sample no.	Sample description	Site	As (mg/kg) Original	As (mg/kg) PM_{10}	Cd (mg/kg) Original	Cd (mg/kg) PM_{10}	Cu (mg/kg) Original	Cu (mg/kg) PM_{10}
Mine tailings	KO-1	Mine tailing dust	Kombat	896	5310	5.0	10	3010	5320
	KAL-1	Mine tailing dust	Berg Aukas	147	347	308	294	142	410
	KAL-2	Mine tailing dust	Berg Aukas	115	127	365	356	132	304
	T20	Mine tailing dust	Tsumeb	4600	4480	25	46	4600	8110
	T21	Mine tailing dust	Tsumeb	5370	4410	26	45	3370	5260
	T22	Mine tailing dust	Tsumeb	727	6150	149	376	2070	3570
	T23	Mine tailing dust	Tsumeb	699	1120	166	523	2520	4370
	T24	Mine tailing dust	Tsumeb	3190	3710	126	217	6530	13,500
Slag dusts	BA13	Zn calciner slag dust	Berg Aukas	1500	596	12	29	575	616
	T2	Ausmelt slag dust	Tsumeb	4910	8190	42	182	6880	11,400
	T4	Ausmelt slag dust	Tsumeb	3800	8600	50	202	6680	13,300
	T5	Dust after slag flotation	Tsumeb	8540	9440	50	63	187,000	87,100
	T19	Slag tailing	Tsumeb	5330	2100	26	44	5150	5700
Smelter dusts	T7	Arsenic dust residue	Tsumeb	118,000	144,000	2100	3050	34,200	36,100
	T8-2	Boiler dust	Tsumeb	115,000	122,000	203	346	54,400	30,200
	T9	Cooling flue gas residue	Tsumeb	257,000	253,000	1160	1500	30,600	19,100
	T16	Bag-house dust	Tsumeb	437,000	580,000	885	653	13,100	4390

Dust category	Sample no.	Mineralogy (XRD)	Pb (mg/kg) Original	Pb (mg/kg) PM_{10}	Sb (mg/kg) Original	Sb (mg/kg) PM_{10}	Zn (mg/kg) Original	Zn (mg/kg) PM_{10}
Mine tailings	KO-1	Dol, Cal, Qtz, Ms, Hem, Ap, Ten*	1900	3850	114	278	664	724
	KAL-1	Dol, Kfs, Cal, Qtz, Des, Wi, Gth, Hem, Sm, Bir, Cer	11,200	29,600	49	101	61,800	157,000
	KAL-2	Dol, Kfs, Cal, Qtz, Des, Hem, Wi, Gth, Sm	9820	21,600	53	97	43,500	47,300
	T20	Dol, Ms, Bt, Qtz, Cal**	3130	2490	77	41	1670	1380
	T21	Dol, Ms, Qtz, Cal**	3940	3370	126	101	1880	1290
	T22	Dol, Kfs, Gp, Ms, Cal, Qtz**	6770	11,300	41	61	5720	15,600
	T23	Dol, Gp, Qtz, Ms, Cal**	8240	11,200	25	30	6450	19,600
	T24	Dol, Ms, Qtz, Cal**	5810	18,000	46	75	5320	8340
Slag dusts	BA13	Mel, Cpx, Ol, Gl, Wi, Cal, Arg	7470	18,200	103	120	62,300	57,600
	T2	Gl, Spl, Ol, Qtz, Dol	24,200	28,300	617	833	48,000	30,000
	T4	Gl, Spl, Ol, Qtz	22,300	28,400	507	791	48,500	30,900
	T5	Gl, Spl, Ol, Cpx, Bn	14,000	12,800	3200	3800	19,600	21,100
	T19	Gl, Ol, Cpx, Qtz, Spl, Dol, Rt	9220	7390	746	919	15,700	14,800
Smelter dusts	T7	Qtz, Gl, Mag, Gp, Jbm, Mim, Sp	119,000	117,000	5620	6600	53,100	55,600
	T8-2	Qtz, Gl, Mul, Ala, Hem, Con, Asl, Cv	32,000	43,700	1400	13,700	21,200	30,000
	T9	Ars, Mul, Gun, Ang, Ala, Hem, Mim, Bi, Gl	52,500	63,700	16,600	27,600	34,700	36,500
	T16	Ars, Cla, Gp, Ang, Qtz, Cv, Gn	39,700	26,000	13,300	14,800	20,000	7930

Abbreviations: Ala – alarsite ($AlAsO_4$), Ang – anglesite ($PbSO_4$), Ap – apatite [$Ca_5(PO_4)_3(OH,F,Cl)$], Arg – aragonite ($CaCO_3$), Ars – arsenolite (As_2O_3), Bi – metallic bismuth, Bir – birnessite (MnO_2), Bn – bornite (Cu_5FeS_4), Bt – biotite [$K(Mg,Fe)_3[AlSi_3O_{10}(OH,F)_2]$], Cal – calcite ($CaCO_3$), Cer – cerussite ($PbCO_3$), Cla – claudetite ($As_2O_3$), Con – conichalcite [$CaCu(AsO_4)(OH)$], Cpr – cuprite ($Cu_2O$), Cpx – clinopyroxene, of hedenbergite composition ($CaFeSi_2O_6$), Cv – covellite (CuS), Des – descloizite [$(Pb,Zn)_2(OH)VO_4$], Dol – dolomite [$CaMg(CO_3)_2$], Duf – duftite [$PbCu(AsO_4)(OH)$], Gl – glass, Gp – gypsum ($CaSO_4 \cdot 2H_2O$), Gth – goethite ($FeOOH$), Gun – gunningite [$(Zn,Mn)SO_4 \cdot H_2O$], Hem – hematite (Fe_2O_3), Jbm – johnbaumite [$Ca_5(AsO_4)_3(OH)$], Kfs – K-feldspar ($KAlSi_3O_8$), Mag – magnetite (Fe_3O_4), Mel – melilite [$(Ca,Na)_2(Al,Mg,Fe)(Si,Al)_2O_7$], Mim – mimetite [$Pb_5(AsO_4)_3Cl$], Ms – muscovite [$KAl_2(Si_3Al)O_{10}(OH,F)_2$], Mul – mullite ($Al_6Si_2O_{13}$), Ol – olivine, mainly of fayalite (Fe_2SiO_4) composition, Prm – pyromorphite [$(Pb,Ca)_5(PO_4)_3Cl$], Py – pyrite (FeS_2), Qtz –quartz (SiO_2), Rt – rutile (TiO_2), Sm – smithsonite ($ZnCO_3$), Sp – sphalerite (ZnS), Spl – spinel [$(Fe^{2+},Mg,Zn)(Fe^{3+},Al,Cr)_2O_4$], Ten – tennantite [$(Cu,Fe)_{12}As_4S_{13}$], Wi – willemite ($Zn_2SiO_4$).

  * SEM/EDS and EPMA detected the presence of pyrite (FeS_2) and cuprite (Cu_2O).

  ** SEM/EDS and EPMA detected the presence of conichalcite, duftite [$PbCu(AsO_4)(OH)$], galena, smithsonite, willemite and Cu sulfides with variable compositions.

of the total contents (*i.e.*, the bioaccessible fraction, BAF). The solid residues, after the extraction tests, were dried at room temperature and analyzed using XRD to determine possible changes in the mineralogical composition during the leaching/extractions.

2.4. Exposure assessment

The calculations of oral exposure were based on adults, particularly on workers, who have been considered as the most highly exposed targets in and around the mining sites and smelter facilities, despite the fact that children also can come into contact with these dust materials in some cases (Fig. 1c). We used a rather conservative value for the dust ingestion rate, corresponding to 50 mg/kg, which is generally used in this kind of exposure assessment (Bierkens et al., 2011). The daily intakes of metal(loid)s obtained were then compared with the tolerable

daily intake (TDI) limits taken from Baars et al. (2001) and Tiesjema and Baars (2009) and calculated for an adult weighing 70 kg. The European Food Safety Authority (EFSA) has recently revised tolerable weekly intake (TWI) for Cd, corresponding to 2.5 μg/kg body weight per day (EFSA, 2009). EFSA also recently concluded that provisional TWI limits for Pb (15 μg/kg body weight) and As (15 μg/kg body weight) are no longer appropriate (EFSA, 2010, 2014); however, for the sake of consistency we used the older values for Pb and As set by Baars et al. (2001).

2.5. Quality control/quality assurance and data treatment

The accuracy of the digestions and subsequent analytical determinations were controlled by parallel analyses of a CCU-1e copper concentrate certified reference material released by the CCRMP-Canadian
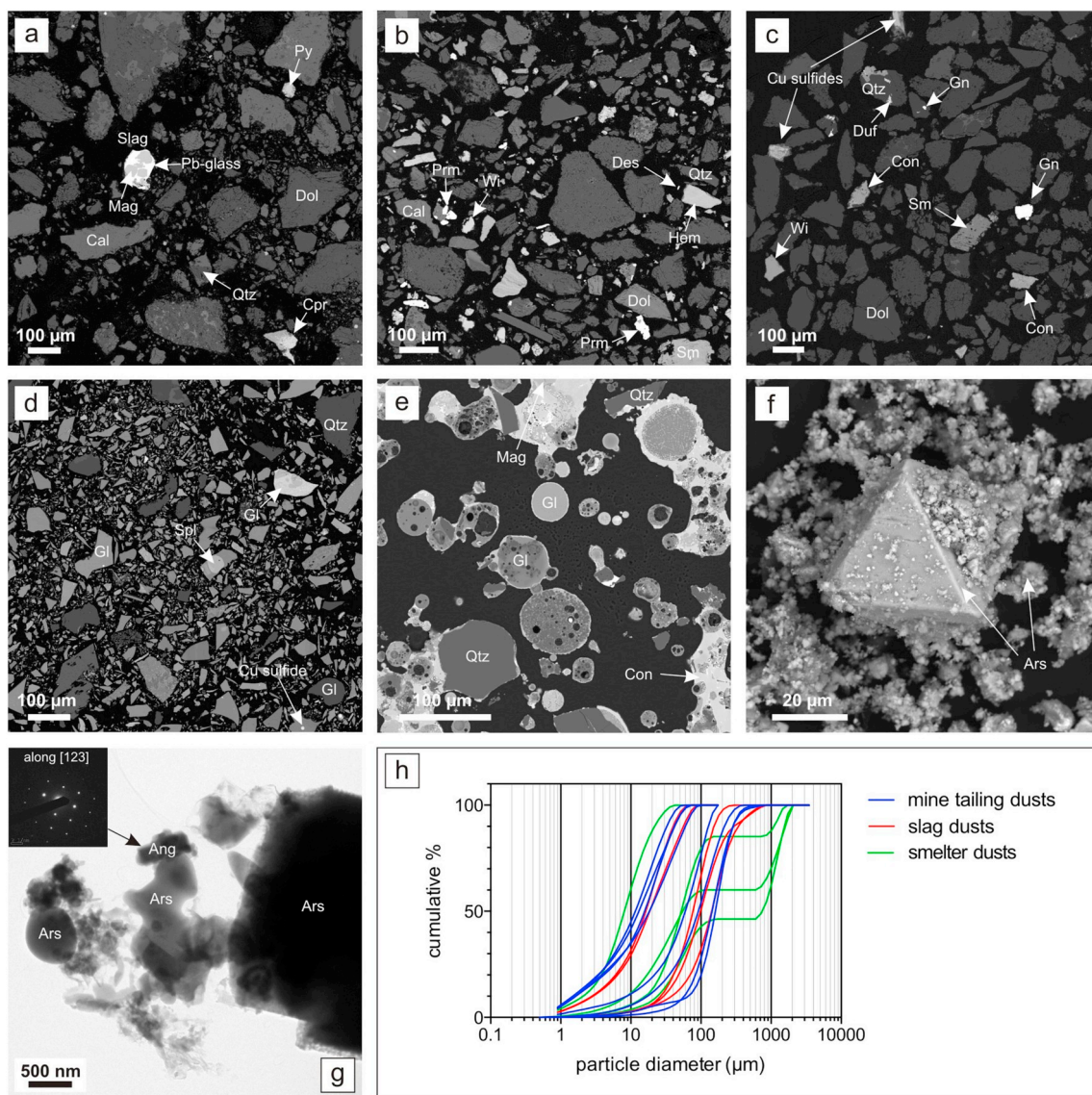
Fig. 2. Micrographs and grain size distribution of the dust samples. (a) Mine tailing dust (Kombat, sample KO-1, polished section, scanning electron microscope [SEM] image in back-scattered electrons, [BSE]) composed predominantly of dolomite, silicates, as well as grains of pyrite, cuprite and slag particles probably originating from re-flotation of Tsumeb slag. (b) Mine tailing dust (Berg Aukas, sample KAL-1, polished section, BSE) predominantly composed of dolomite and calcite, with minor Fe-oxides, quartz, willemite, Pb-Ca phosphates, descloizite and smithsonite. (c) Mine tailing dust (Tsumeb, sample T24, polished section, BSE) composed of dolomite with minor quartz, sulfides (galena, unidentified Cu-sulfides), willemite, smithsonite and arsenates (conichalcite, duftite). (d) Slag dust (Tsumeb, sample T19, polished section, BSE) obtained after slag re-flotation and composed of glass fragments with variable metal(loid) content, with embedded crystals of magnetite and droplets of Cu-sulfides. (e) Copper smelter boiler dust (Tsumeb, sample T8-2, polished section, BSE) composed of droplets of metal(loid)-bearing glass, quartz and magnetite grains, often embedded in a conichalcite matrix. (f) Copper smelter bag-house dust (Tsumeb, sample T16, powder sample, BSE) composed of arsenolite octahedral crystals associated with minuscule arsenolite. (g) Copper smelter bag-house dust (Tsumeb, sample T16, powder sample, transmission electron microscope [TEM] image with associated selected area electron diffraction pattern [SAED]) composed of arsenolite particles of variable grain-size and anglesite. (h) Cumulative grain size curves for individual dust samples.

Abbreviations: Ang – anglesite ($PbSO_4$), Ars - arsenolite (As_2O_3), Cal – calcite ($CaCO_3$), Con – conichalcite [$CaCu(AsO_4)(OH)$], Cpr – cuprite (Cu_2O), Des – descloizite [$(Pb,Zn)_2(OH)VO_4$], Dol – dolomite [$CaMg(CO_3)_2$], Duf – duftite [$PbCu(AsO_4)(OH)$], Gl – glass, Hem – hematite (Fe_2O_3), Mag – magnetite (Fe_3O_4), Ol – olivine, mainly of fayalite (Fe_2SiO_4) composition, Prm – pyromorphite [$(Pb,Ca)_5(PO_4)_3Cl$], Py – pyrite (FeS_2), Qtz –quartz (SiO_2), Sm – smithsonite ($ZnCO_3$), Spl – spinel [$(Fe^{2+},Mg,Zn)(Fe^{3+},Al,Cr)_2O_4$], Wi – willemite ($Zn_2SiO_4$).

Certified Reference Materials project (CANMET, Canada). The accuracy of the analytical determinations in leachates, extracts, and digests was controlled by parallel analyses of the standard reference materials SRM 1640a (Trace elements in natural water) and SRM 1643d (Trace elements in water) released by the National Institute of Standards and Technology (NIST, USA). The quality control/quality assurance (QC/QA) results are reported in Table S1 and indicate good agreement between the measured and certified values. The external reproducibility of the leaching experiments/extractions performed in duplicate varied in the range 0.14–16% relative standard deviation (RSD) (median: 2.67% RSD). All of the data were plotted using Prism 6 software (GraphPad, USA). Prism 6 was also used for the statistical data treatment. Bioaccessible concentration data were log-transformed and one-way ANOVA was used to analyze the differences among groups (mine tailing dusts, slag dusts, smelter dusts). Subsequently, multiple comparisons (Tukey's test) were used to compare pairs of individual sample groups. Binomial sign test was used for comparisons of medians of bioaccessibilities between original dust samples and PM_{10}.

3. Results

3.1. Granulometry and mineralogical composition of the dust samples

The dust samples studied exhibited great variability in their grain-size distributions (Figs. 2h and S2). Grain-sizes for mine tailing dust showed that 90% of the particles were < 300 μm (medians: 13–161 μm). Half of the mine tailing samples were even finer, with a higher proportion in the PM$_{10}$ fraction (36–47%) (Fig. S2a). Except for samples T5 and T19, which originated from slag re-processing by milling and flotation (medians: 16–19 μm), the other slag samples (produced by granulation) were significantly coarser (medians: 77–142 μm). The proportion of PM$_{10}$ was ~30% for the first group and ~3% for the second group of slag dusts, respectively (Fig. S2b). Smelter dusts originating from various stages of flue-gas cleaning technologies were either very fine-grained (sample T16; median: 8 μm, PM$_{10}$ ~63%) or exhibited a bimodal distribution with 43–80% of particles < 100 μm, and the remainder corresponding to the 720–2060 μm size fraction (PM$_{10}$ varied in the 4–12% range) (Fig. S2c). Re-measurement of the grain-size distributions of the separated PM$_{10}$ on representative original samples of each category indicated the efficiency of the sieving procedure (Fig. S2d).

A combination of XRD, SEM/EDS, TEM/EDS and EPMA indicated complex mineralogical compositions of dust samples, reflecting the local geological conditions of the individual deposits as well as the technological processes used (ore processing, smelting, smelter flue-gas cleaning) (Table 1, Fig. 2). All of the mine tailing dusts contained gangue minerals (carbonates [dolomite, calcite], quartz and micas) as well as secondary phases (*e.g.*, hematite) (Table 1, Figs. 2a, b, c and S3; see structural formulae of the individual minerals in legend of Table 1). These materials also contained residual metal(loid)-bearing phases such as sulfides and sulfosalts (pyrite, Cu-sulfides, galena, tennantite; Fig. 2a, c), oxides (cuprite; Fig. 2a), carbonates (smithsonite; Fig. 2b), various metal arsenates, phosphates and vanadates (*e.g.*, conichalcite, pyromorphite, descloisite; Fig. 2b, c), plus silicates (willemite; Fig. 2b) (Fig. S3). Interestingly, a few smelter slag particles have also been found in the tailing material from Kombat, despite the fact that no metallurgy was active at this site (Fig. 2a). We speculate that the froth flotation technology at Kombat was also partly used for slag reprocessing at the time of insufficient flotation capacities at Tsumeb, given the fact that the same company, Ongopolo Mining and Processing Ltd., historically owned both mines. Whereas the Zn calciner slag dust from Berg Aukas was mainly composed of high-temperature phases (melilite, clinopyroxene, olivine, Zn-bearing glass, willemite) and partly mixed with wind-blown geogenic carbonates, the mineralogy of the Tsumeb slag dusts corresponded well to previously published data (Ettler et al., 2009; Jarošíková et al., 2017). Due to quenching of the slag melt, the slag dusts from Tsumeb were predominantly composed of metal(loid)-bearing glass, with minor proportions of olivine, spinel-family phases,

clinopyroxene, sulfide droplets and windblown geogenic minerals such as quartz or carbonates (Table 1, Figs. 2d and S3). Smelter dusts consisted of unmelted/partially melted residual phases from the furnace charge (*e.g.*, quartz) and phases formed during the cooling of the flue gas: droplets of quenched slag-like material (glass, mullite, sulfides) (Figs. 2e and S3), as well as phases formed by condensation from the vapor (particularly binding volatile elements such as As, Sb, Pb, Zn: arsenolite, claudetite, arsenates, gunningite) (Table 1, Figs. 2f, g and S3). Smelter dusts from later stages of flue gas cooling (T9, T16) contained a high proportion of the fine-grained fraction, composed of relatively soluble phases such as Sb-bearing arsenolite (Figs. 2f, g, h and S2; see also Jarošíková et al., 2018).

3.2. Chemical composition of the dust samples

The concentrations of metal(loid)s in original dust samples and their PM$_{10}$ fractions are reported in Table 1. In terms of absolute concentrations, As, Cu, Pb, and Zn were the principal contaminants (ranging from hundreds of mg/kg to tens of wt%). Arsenic, for example, varied between 115 mg/kg and 58 wt%; in contrast, Cd and Sb were found in lower concentrations (5–3050 mg/kg, and 25–27,600 mg/kg, respectively). The bulk metal(loid) concentrations generally decreased in the following order: smelter dusts > slag dusts > mine tailing dusts (Table 1). For the majority of samples, metal(loid) concentrations were higher for PM$_{10}$ than for the original dusts, which was in good agreement with the previous studies about the distribution of contaminants among various particle size fractions of contaminated soils, dusts and aerosols (Juhasz et al., 2011; Csavina et al., 2012 and references therein; Ettler et al., 2014). However, there were still numerous exceptions, which seem to be related to the mineralogical composition and partitioning of contaminants among the various phases. For example, the T19 slag tailing dust exhibited higher concentrations of As, Pb, and Zn in the original sample than in the PM$_{10}$, because of their binding predominantly in larger glass fragments (Table 1, Fig. 2d; Jarošíková et al., 2017). Likewise, the PM$_{10}$ of bag-house dust (T16) exhibited higher concentrations of As and Sb, because these metalloids also formed submicrometric crystals of Sb-bearing As$_2$O$_3$ (arsenolite, claudetite) (Fig. 2f, g), whereas metals (Cd, Cu, Pb, Zn) were predominantly bound in larger fragments of metallic sulfides and metal-arsenates (see a detailed description in Jarošíková et al., 2018).

3.3. Leaching properties and dust classification

The EN 12457-2 regulatory leaching test showed striking differences in contaminant leaching from the three groups of dust materials studied (Fig. 3, Table S2). Equilibrium pH of the leachates obtained indicated near neutral to slightly alkaline conditions for the majority of the samples (6.6–8.2); in contrast, several smelter dust samples were acidic, yielded a low equilibrium pH of the leachate (1.8–5.9), likely
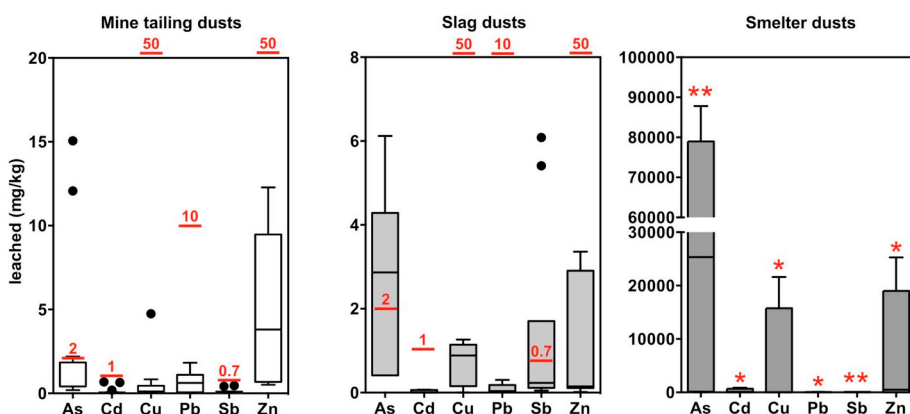

Fig. 3. Tukey box-plot diagrams showing variability of leached concentrations of As, Cd, Cu, Pb, Sb and Zn for individual dust samples and comparisons with EU limit values for non-hazardous wastes (EU, 2002). The data were plotted from replicated leaching tests. One asterisk indicates that at least one of the dust samples exceeded the EU leaching limit for hazardous wastes; two asterisks symbol indicates that all the dust samples in the given category exceeded this limit.

due to their formation within the smelter's flue gas stream enriched in SO_2 (Table S2).

In terms of contaminant leaching, mine tailing dusts generally exhibited low concentration of leached metals and Sb (maximum values in mg/kg: Cd 0.67, Cu 2.79, Pb 1.37, Sb 0.44, Zn 10.86), accounting for < 1.4% of their total content. However, As leaching exceeded the limit value for non-hazardous waste in the case of two samples (3.4 to 4.3×) (Fig. 3, Table S2). For the slag dust materials, the leached concentrations accounted for < 0.18% of the total concentrations. The leaching properties of slag dusts indicated that leached concentrations of metals were below the EU limit values for non-hazardous wastes, but exceeded them in the case of As (up to 3×; n = 3; Table S2). Moreover, sample T5 slightly exceeded the limit value for hazardous waste involving Sb (5.75 mg/kg; Fig. 3, Table S2). Compared to mine tailing and slag dusts, samples from smelter flue-gas cleaning systems exhibited significantly higher leaching rates of contaminants (up to 34% As, 73% Cd, 70% Cu, 0.2% Pb, 0.72% Sb and 73% Zn; each of the total) (Table S2). Arsenic and Sb were the most critical contaminants, notably exceeding the limit values for hazardous waste (1.1–3500× and 1.8–19×, respectively). Moreover, for other smelter dust samples, at least one of the metallic contaminants also exceeded the limit for hazardous waste (Fig. 3, Table S2). According to EU legislation (EU, 2002), none of the smelter dust samples met the criteria for landfilling at a controlled hazardous waste landfill, and would have needed special treatment (solidification/stabilization) *prior* to their disposal.

3.4. Contaminant bioaccessibility and exposure estimates

Bioaccessible concentrations of metal(loid)s from the original dust samples and the PM_{10} fractions are reported in Fig. 4 and Table S3. One-way ANOVA performed on log-transformed bioaccessible metal(loid) concentrations rejected the hypothesis that all the three groups belong to the same population for As, Cd (bulk dusts only), Pb (bulk dusts only) and Sb (p < 0.05) (Table S4). Multiple comparisons (Tukey's test) confirmed that the smelter dusts were statistically different compared to the mine tailing dusts in case of As and Sb bioaccessibilities for both bulk dusts and PM_{10} fractions and in case of Pb for bulk dusts only (Table S4). Smelter dusts were also statistically different compared to slag dusts in case of As and Cd (bulk dusts only) (Table S4). The median values of the bioaccessibilities were systematically higher for the PM_{10} fraction than for the original samples (Fig. 4, Table S3); this finding was also statistically confirmed by a sign test (p < 0.0001). Overall, the bioaccessible concentrations and median BAF values ordered as: mine tailing dusts < slag dusts < smelter dusts (Fig. 4, Table S3).

The mineralogical analysis of the residues after the extraction in SGF indicated changes in the phase compositions for some of the samples (Fig. S3). In the case of mine tailing dusts, due to the highly acidic conditions calcite almost completely disappeared and dolomite also partly dissolved. Tennantite disappeared from the XRD pattern (sample KO-1) and willemite, descloizite and metal carbonates also substantially dissolved (sample KAL-1) (Fig. S3). In the T19 slag dust sample, we detected that some of the geogenic phases were dissolved after the extraction in SGF (dolomite, rutile) and clinopyroxene also partly dissolved due to the highly acidic conditions and the presence of a chelating agent (glycine). Given the fact that the raised background of the XRD pattern approximately at the 20–40° 2-theta interval (indicative for glass) was not very high in the dust residue, we also hypothesize that metal(loid)-bearing glass was significantly etched during the extraction in SGF (Fig. S3). The most significant changes in the mineralogical compositions after extraction were reported for the smelter dusts (Fig. S3). Several phases such as gypsum (T7, T16) as well as numerous metal arsenates (johnbaumite, mimetite, alarsite) (T7, T9), mullite and gunningite (T9) almost completely disappeared and arsenolite was also substantially dissolved (T9, T16) (Fig. S3) - leading to especially high levels of bioaccessible As.

The exposure estimates which are based on the assumption of a daily dust intake of 50 mg are reported in Table 2 and indicate that the elements of risk are primarily As, Pb and Cd, whereas other contaminants exhibited calculated exposures far below the TDI values. Mine tailing dusts only exceeded the TDI limit for As in a single sample (T24) for both the original dust and PM_{10} fraction (up to 1.6×); several PM_{10} samples exceeded the TDI limit for Pb (up to 3.5×; n = 5). High As exposure was also estimated for the slag dust samples from Tsumeb for both the original dusts and PM_{10} (exceeding by up to 3.4× the TDI value, n = 3) (Table 2). Lead was also a key contaminant in the case of slag dusts (2 original samples and all PM_{10} fractions), with daily intakes exceeding up to 4× the TDI limits (Table 2). The most hazardous materials were the smelter dusts with extremely high calculated exposures, far exceeding the TDI for As (30× to 320×), Pb (up to 8×) and Cd (up to 2×); the calculated intakes of As and Pb from PM_{10} were approximately twice as high as those from the original dusts (Table 2). Despite the conservative dust daily intake (50 mg/day), which is probably highly underestimated for the dry and dusty environments in northern Namibia, it can be concluded that smelter dust materials and granulated slag disposed on the dumps represent a significant source for potential exposure to toxic metal(loid)s, particularly As and Pb.

4. Discussion

The bulk concentrations of metal(loid)s were generally higher for slags and smelter dusts than for mine tailings (Table 1). Up to 58 wt% As, 2920 mg/kg Cd, 18.7 wt% Cu, 11.9 wt% Pb, 2.76 wt% Sb and 6.23 wt% Zn were found in the dusts studied; this is all in agreement with previous investigations of mining- and smelter-derived materials from the study area (*e.g.*, Ettler et al., 2009; Mapani et al., 2010; Sracek et al., 2014a, 2014b; Jarošíková et al., 2017, 2018; Kříbek et al., 2018) as well as from other mining/smelting districts (Morrison and Gulson, 2007; Ghorbel et al., 2010; Boisa et al., 2013; Ettler et al., 2014; Morrison et al., 2016; Drahota et al., 2018; Ettler et al., 2018). It is important to recall that smelter dusts were substantially enriched in highly volatile elements such as As, Cd, Pb and Sb (Table 1) in accordance with previously published data on chemical and mineralogical compositions of smelter flue dusts (Romero et al., 2008; Skeaff et al., 2011; Jarošíková et al., 2018).

Bulk metal(loid) concentrations generally increased with decreasing particle size, as have previously been reported for contaminated soils (Juhasz et al., 2011) and technological materials such as slags (Morrison and Gulson, 2007; Morrison et al., 2016). However, our data showed that there are some exceptions to this rule and that metal(loid) concentrations might decrease as a function of decreasing particle size (Table 1). This phenomenon has also been observed for some elements in slags (Zn: Morrison et al., 2016), smelter flue dusts (Co: Ettler et al., 2014), smelter-derived aerosols (Pb: Uzu et al., 2011), and even soils (Co, Mn, Zn: Kastury et al., 2018). This can be explained by either specific binding of these elements in solid phases (which form larger fragments in a given material) or by overall variability in the mineralogical composition.

The bioaccessibility of contaminants is highly dependent on the mineralogy. The combination of mineralogical investigations with *in vivo* experiments indicated that: Pb associated with carbonates and Mn-oxides are the most bioavailable *via* ingestion; Pb associated to phosphates, oxides and Fe-oxides show an intermediate bioavailablity; and Pb sulfides, silicates and vanadates are the least bioavailable (Plumlee and Morman, 2011 and references therein). *In vitro* experiments conducted by Bosso and Enzweiler (2008) on pure Pb-bearing phases reported that Pb carbonates and Pb oxides yielded almost 100% of Pb bioaccessible, whereas Pb bioaccessibilities in acidic SGF were < 7% for galena and pyromorphite. Numerous metal(loid)-bearing phases found in our dusts show U- or V-shaped pH-dependent solubilities and are expected to dissolve to a greater extent under the highly acidic conditions of SGF (for comparisons see the modeled data in Jarošíková
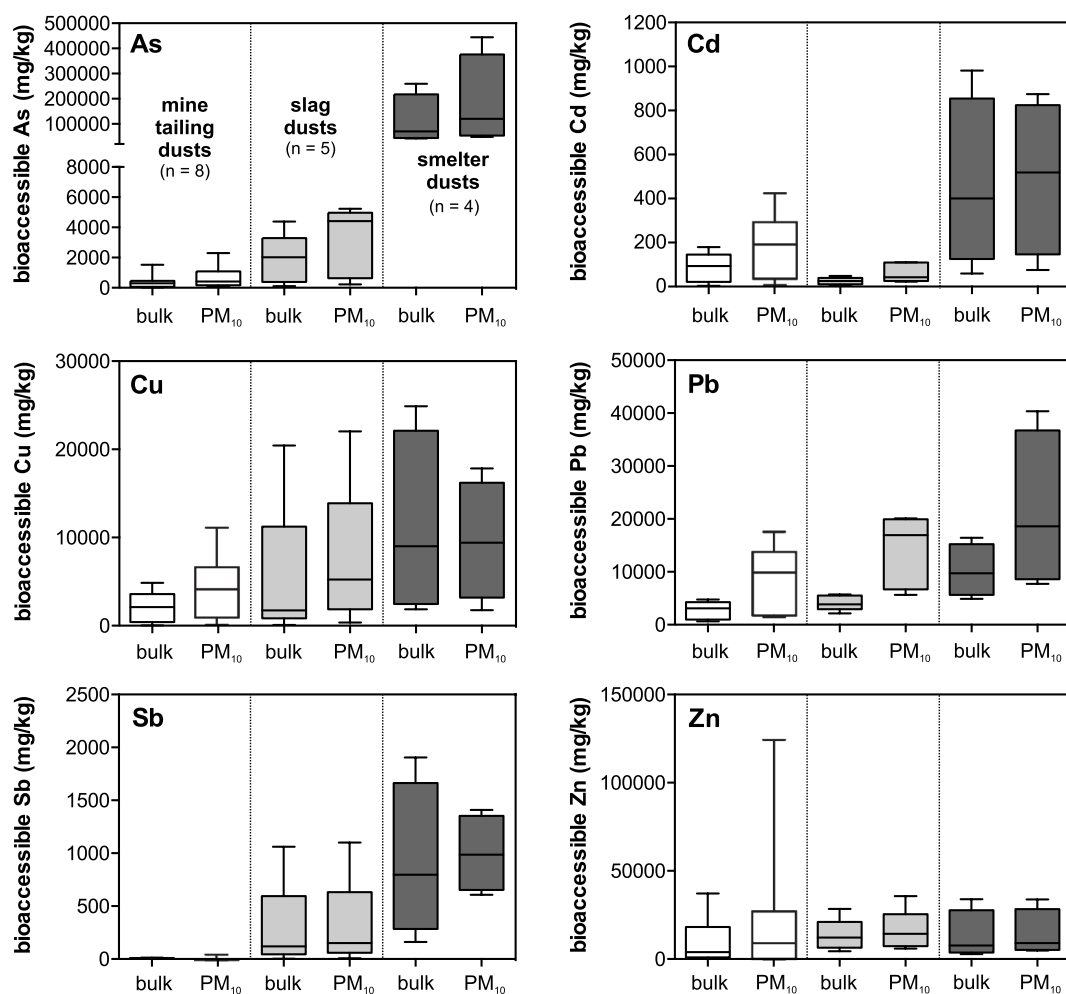
Fig. 4. Bioaccessible concentrations of As, Cd, Cu, Pb, Sb and Zn as Tukey box-plot diagrams and comparisons between the bulk dust samples and PM$_{10}$ fractions.

et al., 2017, 2018). Thus, it is possible that, apart from dissolution of highly soluble phases (*e.g.*, cerussite and descloisite), also less soluble phases such as galena or metal-arsenates can, to a certain degree, become sources of bioaccessible Pb due to their higher dissolution at low pH values.

Molina et al. (2013) conducted *in vivo* experiments (with rats) as well as *in vitro* extractions on variable Zn-bearing compounds. Their study found that the bioavailability and bioaccessibility decreased as follows: Zn-rich mine waste > hydrozincite [$Zn_5(CO_3)_2(OH)_6$] > hemimorphite [$Zn_4(Si_2O_7)(OH)_2 \cdot H_2O$] > zincite (ZnO) ≈ smithsonite (ZnCO$_3$) ≫ sphalerite (ZnS). In body fluids, particularly high dissolution was suggested for gunningite (Gieré et al., 2006), a condensation product also found in one of our smelter dust samples (T9). Nevertheless, our data indicate that the bioaccessibility of Zn seems to be less mineralogy-dependent compared to the other contaminants (Fig. 4). According to the ANOVA and Kruskal-Wallis tests (p < 0.05), the differences between the individual groups of samples were not statistically significant for Zn. Exceptionally high Zn bioaccessibility was observed only for sample KAL-1 due to the substantial dissolution of primary willemite and descloisite (Figs. 4 and S3; Table S3).

Metal(loid)-rich glass and inclusions of metallic sulfides are the main sources of bioaccessible contaminants for slag dusts. Previous research devoted to granulated slags from this area showed that up to 2.3 wt% As, 0.09 wt% Cd, 5.5 wt% Cu, 17.4 wt% Pb and 13.0 wt% Zn can be bound in the glass fragments (Ettler et al., 2009; Jarošíková et al., 2017). It is also known that in the smaller grain-size fractions of slags, a higher percentage of metal-bearing inclusions are being

"liberated" and "accessible" for leaching (Morrison et al., 2016); this phenomenon also reflected the higher bioaccessibilities in PM$_{10}$ compared to bulk slag dusts (Fig. 4, Table S3).

Apart from highly soluble arsenolite, which is a key host of As in smelter dust samples (Table 1, Fig. 2; *cf.* Skeaff et al., 2011; Jarošíková et al., 2018), variable arsenates, unstable under highly acidic conditions, are also responsible for high values of bioaccessible As in the majority of the smelter dusts as well as in mine tailing dust sample T24 (also see similar results in Meunier et al., 2010).

The studied mine tailing and slag disposal sites are not covered nor sealed and are exposed to wind erosion, leading to the previously reported contamination of soils and vegetation, including crops (Mileusnic et al., 2014; Mapani et al., 2014; Kříbek et al., 2016, 2018). However, the majority of disposal sites are fenced (Kombat) and/or located in restricted industrial zones (Tsumeb) (Figs. 1 and S1), where access by the local population is limited. At Berg Aukas, several measures have partly followed the recommendations issued from previous studies and agricultural fields were moved from those areas directly affected by windblown contamination from the tailing dams (Mapani et al., 2010). However, in the context of direct exposure to the dust particles, Berg Aukas still represents a problem due to the easily accessible slag dump and mine tailing dams that are located close to the dwellings of local residents (Fig. S1).

Very special care should be taken in the case of smelter dust materials from the Tsumeb smelter site, because they all exceed the leaching limits for hazardous wastes (Table S2, Fig. 3). Furthermore, before landfilling, they should either undergo further chemical

Table 2
Calculated daily intakes for individual contaminants in µg/day, assuming a dust intake of 50 mg/kg (mean value for original dusts, n = 2; single value for PM_{10} fractions), and comparisons with background exposure (BE) and tolerable daily intake (TDI) limits for a 70-kg adult. Values exceeding TDI are indicated in bold.

Code	As		Cd		Cu		Pb		Sb		Zn	
BE[*] (µg/kg/day)	0.3		0.22		30		0.6		0.4		300	
BE (µg/70 kg/day)	21		15.4		2100		42		28		21,000	
TDI[*] (µg/kg/day)	1		0.5		140		3.6		6		500	
TDI (µg/70 kg/day)	70		35		9800		252		420		35,000	
	Original	PM_{10}	Original	PM_{10}	Original	PM_{10}	Original	PM_{10}	Original	PM_{10}	Original	PM_{10}
Mine tailing dusts												
KO-1	20	63	0.2	0.4	73	233	33	131	0.7	2.8	11	30
KAL-1	2.5	10	7.9	11	3.1	10	216	**885**	0.2	0.1	1870	6250
KAL-2	1.3	2.9	9.0	13	2.3	8.4	168	**570**	0.2	0.1	1130	1620
T20	7.0	7.5	1.1	1.8	197	370	47	77	0.3	0.2	43	43
T21	10	11	1.1	1.8	130	241	57	84	0.3	0.3	47	40
T22	24	31	5.5	15	95	168	209	**500**	0.5	0.3	270	655
T23	22	30	5.4	21	116	190	239	**498**	0.2	0.6	227	770
T24	**77**	**115**	4.1	7.9	244	560	142	**740**	0.2	0.5	166	327
Slag dusts												
BA13	5.1	11	0.4	1.1	4.9	18	184	**845**	0.2	0.4	1420	1790
T2	**101**	**235**	1.3	5.4	79	262	**265**	**1010**	6.3	8.4	610	715
T4	**110**	**221**	1.5	5.5	87	287	**285**	**985**	6.0	7.6	690	760
T5	**219**	**262**	2.4	2.1	1020	1100	191	**386**	53	55	417	437
T19	34	53	0.7	1.4	101	169	106	**282**	4.3	5.5	222	299
Smelter dusts												
T7	**2530**	**3550**	24	**34**[**]	214	374	**820**	**2020**	33	71	457	590
T8-2	**2110**	**2430**	3.0	3.7	685	570	246	**565**	8.1	39	141	241
T9	**4520**	**8500**	49[**]	44[**]	1245	890	389	384	47	30	1700	1700
T16	**13,000**	**22,300**	16	18	93	88	**585**	**1290**	96	59	318	317

[*] Defined in Baars et al. (2001) except for Sb, which is defined in Tiesjema and Baars (2009).
[**] Values exceeding TDI defined by EFSA (2009): 0.357 µg/kg/day, 25 µg/70 kg/day.

stabilization and/or solidification, or be reused in the smelting process. The risk of inhalation/ingestion is currently minimized by the safety measures taken by the operator of the smelter (DPMT Ltd.); all of the staff wear obligatory mouth filters/masks during the handling of dust materials or when moving in the operating smelter working areas. Moreover, roads in the area of the smelter are regularly water-sprayed to limit dust dispersion. Despite this, a preliminary biomonitoring study, using urine (n = 154) and blood (n = 148) of people living in the Tsumeb area indicated that more than one fifth of subjects exceeded the WHO limit for blood Pb (10 µg/dL) and one in six persons exceeded the WHO guideline levels for As in urine (50 µg/L) (Mapani et al., 2011). The highest contaminant values in blood and urine were recorded for persons living or working in either the northern industrial zone or in western suburb of Tsumeb, close to the abandoned mining area and smelter complex (Mapani et al., 2011). Our bioaccessibility data confirm a particularly high risk related to the ingestion of slag and smelter dusts, especially due to the high values of calculated daily intake for As, Pb and Cd. The approach adopted in this study corresponds to a "worse-case" scenario (*i.e.*, only highly acidic gastric conditions were considered); however, we are aware that the dust ingestion rate of 50 mg/day used for our model's calculations were highly conservative and the ingestion rates could be much higher in the dusty environments of smelter areas. To fully understand the occupational exposure of workers in the smelter area and the population living near the abandoned mines in the district studied, a more complex human health risk assessment (Swartjes and Cornelis, 2011; Reis et al., 2014), which would combine ingestion, inhalation and dermal exposure with on-site dust monitoring, would be needed. Detailed biomonitoring studies with greater numbers of subjects and comparable to those recently conducted in Kabwe, a Zambian town highly polluted by Pb-Zn mining/smelting activities (Yabe et al., 2015, 2018; Bose-O'Reilly et al., 2018) would be suitable to better describe the sources and pathways of metal(loid) contaminants and their effects on the local population.

5. Conclusions

This study focused on the oral bioaccessibility of As, Cd, Cu, Pb, Sb and Zn in bulk samples and separated PM_{10} fractions of mine tailing, slag and smelter dusts from three old mining and smelting districts of northern Namibia (Kombat, Berg Aukas, Tsumeb). An integrated approach involving a combination of physico-chemical and mineralogical characterization as well as leaching/extraction tests indicated that the amount of bioaccessible metal(loid)s increased as follows: mine tailing dusts < slag dusts ≪ smelter dusts. Extremely high As and Pb bioaccessibilities in the smelter dusts were caused by the presence of highly soluble phases such as arsenolite and metal-arsenates, unstable under the acidic conditions of simulated gastric fluid.

Despite rather conservative assumptions (an adult of 70 kg, a dust ingestion rate of 50 mg/day), the exposure estimates proved that As, Pb and to a lesser extent also Cd significantly exceeded tolerable daily intake limits of these contaminants for some slag dusts and especially for the smelter dust samples. Highly bioaccessible metal(loid)s demonstrate that careful handling of these materials as well as the currently adopted safety measures (mouth filters) are necessary to reduce the smelter staff's exposure to contaminated dust. However, other environmental management strategies are still needed at the freely accessible abandoned old slag deposits at Tsumeb, where slag dusts exhibited highly bioaccessible As and Pb. The substantial exposure risk is also related to the unfenced mine tailing dams and slag deposits at Berg Aukas, which are located in close proximity to the local population and where PM_{10} dust fractions exhibited high Pb bioaccessibilities.

Appendix A. Supplementary data

Supplementary data to this article can be found online at https:// doi.org/10.1016/j.envint.2018.12.027.

References

Alpofead, J.A.H., Davidson, C.M., Littlejohn, D., 2016. Oral bioaccessibility tests to measure potentially toxic elements in inhalable particulate matter collected during routine air quality monitoring. Anal. Methods 8, 5466–5474. https://doi.org/10. 1039/c6ay01403h.

Alpofead, J.A.H., Davidson, C.M., Littlejohn, D., 2017. A novel two-step sequential bioaccessibility test for potentially toxic elements in inhaled particulate matter transported into the gastrointestinal tract by mucociliary clearance. Anal. Bioanal. Chem. 409, 3165–3174. https://doi.org/10.1007/s00216-017-0257-2.

Baars, A.J., Theelen, R.M.C., Janssen, P.J.C.M., Hesse, J.M., van Apeldoorn, M.E., Meijerink, M.C.M., Verdam, L., Zeilmaker, M.J., 2001. Re-evaluation of human-tox-icological maximum permissible risk levels. RIVM report 711701025, Bilthoven, the Netherlands.

Banza, C.L.N., Nawrot, T.S., Haufroid, V., Decrée, S., De Putter, T., Smolders, E., Kabyla, B.I., Luboya, O.N., Ilunga, A.N., Mutombo, A.M., Nemery, B., 2009. High human exposure to cobalt and other metals in Katanga, a mining area of the Democratic Republic of Congo. Environ. Res. 109, 745–752. https://doi.org/10.1016/j.envres. 2009.04.012.

Bierkens, J., Van Holderbeke, M., Cornelis, C., Torfs, R., 2011. Exposure through soil and dust ingestion. In: Swartjes, F.A. (Ed.), Dealing with Contaminated Sites. Springer Science + Business Media B.V, Berlin, pp. 261–286.

Boisa, N., Bird, G., Brewer, P.A., Dean, J.R., Entwistle, J.A., Kemp, S.J., Macklin, M.G., 2013. Potentially harmful elements (PHEs) in scalp hair, soil and metallurgical wastes in Mitrovica, Kosovo: the role of oral bioaccessibility and mineralogy in human PHE exposure. Environ. Int. 60, 56–70 (https://org.doi/j.envint.2013.07.014).

Boisa, N., Elom, N., Dean, J.R., Deary, M.E., Bird, G., Entwistle, J.A., 2014. Development and application of an inhalation bioaccessibility method (IBM) for lead in the PM$_{10}$ size fraction of soil. Environ. Int. 70, 132–142. https://doi.org/10.1016/j.envint. 2014.05.021.

Bose-O'Reilly, S., Yabe, J., Makumba, J., Schutzmeier, P., Ericson, B., Caravanos, J., 2018. Lead intoxicated children in Kabwe, Zambia. Environ. Res. 165, 420–424. https:// doi.org/10.1016/j.envres.2017.10.024.

Bosso, S.T., Enzweiler, J., 2008. Bioaccessible lead in soils, slag, and mine wastes from abandoned mining district in Brazil. Environ. Geochem. Health 30, 219–229. https:// doi.org/10.1007/s10653-007-9110-4.

Brown, J.S., Gordon, T., Price, O., Asgharian, B., 2013. Thoracic and respirable particle definitions for human health risk assessment. Part. Fibre Toxicol. 10, 12. https://doi. org/10.1186/1743-8977-10-12.

Carvalho, T.C., Peters, J.I., Williams III, R.O., 2011. Influence of particle size on regional lung deposition – what evidence is there? Int. J. Pharm. 406, 1–10. https://doi.org/ 10.1016/j.ijpharm.2010.12.040.

Cheyns, K., Banza, C.L.N., Ngombe, L.K., Asosa, J.A., Haufroid, V., De Putter, T., Nawrot, T., Kimpanga, C.M., Numbi, O.L., Ilunga, B.K., Nemery, B., Smolders, E., 2014. Pathways of human exposure to cobalt in Katanga, a mining area of the D. R. Congo. Sci. Total Environ. 490, 313–321. https://doi.org/10.1016/j.scitotenv.2014.05.014.

Csavina, J., Field, J., Taylor, M.P., Gao, S., Landázuri, A., Betterton, E.A., Sáez, E.A., 2012. A review on the importance of metals and metalloids in atmospheric dust and aerosol from mining operations. Sci. Total Environ. 433, 58–73. https://doi.org/10. 1016/j.scitotenv.2012.06.013.

Denys, S., Caboche, J., Tack, K., Rychen, G., Wragg, J., Cave, M., Jondreville, C., Feidt, C., 2012. In vivo validation of the unified BARGE method to assess the bioaccessibility of arsenic, antimony, cadmium, and lead in soils. Environ. Sci. Technol. 46, 6252–6260. https://doi.org/10.1021/es3006942.

Deshommes, E., Tardif, R., Edwards, R., Sauvé, S., Prévost, M., 2012. Experimental de-termination of the oral bioavailability and bioaccessibility of lead particles. Chem. Cent. J. 6, 138. https://doi.org/10.1186/1752-153X-6-138.

Drahota, P., Raus, K., Rychlíková, E., Rohovec, J., 2018. Bioaccessibility of As, Cu, Pb, and Zn in mine waste, urban soil, and road dust in the historical mining village of

Kaňk, Czech Republic. Environ. Geochem. Health 40, 1495–1512. https://doi.org/10. 1007/s10653-017-9999-1.

EFSA, 2009. Cadmium in food. Scientific opinion of the Panel on Contaminants in the Food Chain on a request from the European Commission on cadmium in food. EFSA J. 2009 (980), 1–139.

EFSA, 2010. Scientific opinion on lead in food. EFSA J. 8 (4), 1570. https://doi.org/10. 2903/j.efsa.2010.1570.

EFSA, 2014. Dietary exposure to inorganic arsenic in the European population. EFSA J. 12 (3), 3597. https://doi.org/10.2903/j.efsa.2014.3597.

EN 12457, 1999. Characterization of Waste – Leaching – Compliance Test for Leaching of Granular Waste Materials and Sludges, part 2. CEN, Brussels.

Entwistle, J.A., Hunt, A., Boisa, N., Dean, J.R., 2017. Enhancing the interpretation of in vitro bioaccessibility data by using computer controlled scanning electron micro-scopy (CCSEM) at the individual particle level. Environ. Pollut. 228, 443–453. https://doi.org/10.1016/j.envpol.2017.03.050.

Ettler, V., 2016. Soil contamination near non-ferrous smelters: a review. Appl. Geochem. 64, 56–74. https://doi.org/10.1016/j.envpol.2014.04.035.

Ettler, V., Johan, Z., Kříbek, B., Šebek, O., Mihaljevič, M., 2009. Mineralogy and en-vironmental stability of slags from the Tsumeb smelter, Namibia. Appl. Geochem. 24, 1–15. https://doi.org/10.1016/j.apgeochem.2008.10.003.

Ettler, V., Vítková, M., Mihaljevič, M., Šebek, O., Klementová, M., Veselovský, F., Vybíral, P., Kříbek, B., 2014. Dust from Zambian smelters: mineralogy and contaminant bioaccessibility. Environ. Geochem. Health 36, 919–933. https://doi.org/10.1007/ s10653-014-9609-4.

Ettler, V., Johan, Z., Kříbek, B., Veselovský, F., Mihaljevič, M., Vaněk, A., Penížek, V., Majer, V., Sracek, O., Mapani, B., Kamona, F., Nyambe, I., 2016. Composition and fate of mine- and smelter-derived particles in soils of humid subtropical and hot semi-arid areas. Sci. Total Environ. 563–561, 329–339. https://doi.org/10.1016/j. scitotenv.2016.04.133.

Ettler, V., Polák, L., Mihaljevič, M., Ratié, G., Garnier, J., Quantin, C., 2018. Oral bioaccessibility of inorganic contaminants in waste dusts generated by laterite Ni ore smelting. Environ. Geochem. Health 40, 1699–1712. https://doi.org/10.1007/ s10653-016-9875-4.

EU, 2002. Council decision of 19 December 2002 establishing criteria and procedures for the acceptance of waste at landfills pursuant to article 16 of and annex II to directive 1999/31/EC. Off. J. Eur. Communities L11 (2002), 27–49.

Frimmel, H.E., Deane, J.G., Chadwick, P.J., 1996. Pan-African tectonism and the geneis of base metal sulfide deposits in the northern foreland of the Damara Orogen, Namibia. In: Sangster, D.F. (Ed.), Carbonate-hosted Lead-zinc Deposits. Spec. Publ. No. 4 Society of Economic Geology, Littleton, pp. 204–217.

Ghorbel, M., Munoz, M., Courjault-Radé, P., Destingeville, C., de Perseval, P., Souissi, R., Souissi, F., Ben Mammou, A., Abdeljaouad, S., 2010. Health risk assessment for human exposure by direct ingestion of Pb, Cd, Zn bearing dust in the former mi-ners'village of Jebel Ressas (NE Tunisia). Eur. J. Mineral. 22, 639–649. https://doi. org/10.1127/0935-1221/2010/0022-2037.

Gieré, R., Blackford, M., Smith, K., 2006. TEM study of PM$_{2.5}$ emitted from coal and tire combustion in a thermal power station. Environ. Sci. Technol. 40, 6235–6240. https://doi.org/10.1021/es060423m.

Gražulis, S., Daškevič, A., Merkys, A., Chateigner, D., Lutterotti, L., Quirós, M., Serebryanaya, N.R., Moeck, P., Downs, R.T., Le Bail, A., 2012. Crystallography Open Database (COD): an open-access collection of crystal structures and platform for world-wide collaboration. Nucleic Acids Res. 40, D420–D427. https://doi.org/10. 1093/nar/gkr900.

Harvey, P.J., Taylor, M.P., Kristensen, L.J., Grant-Vest, S., Rouillon, M., Wu, L., Handley, H.K., 2016. Evaluation and assessment of the efficacy of an abatement strategy in a former lead smelter community, Boolaroo, Australia. Environ. Geochem. Health 38, 941–954. https://doi.org/10.1007/s10653-015-9779-8.

Jarošíková, A., Ettler, V., Mihaljevič, M., Kříbek, B., Mapani, B., 2017. The pH-dependent leaching behaviour of slags from various stages of a copper smelting process: en-vironmental implications. J. Environ. Manag. 187, 178–186. https://doi.org/10. 1016/j.envman.2016.11.037.

Jarošíková, A., Ettler, V., Mihaljevič, M., Drahota, P., Culka, A., Racek, M., 2018. Characterization and pH-dependent environmental stability of arsenic trioxide-con-taining copper smelter flue dust. J. Environ. Manag. 209, 71–80. https://doi.org/10. 1016/j.envman.2017.12.044.

Juhasz, A.L., Weber, J., Smith, E., 2011. Impact of soil particle size and bioaccessibility on children and adult lead exposure in peri-urban contaminated soils. J. Hazard. Mater. 186, 1870–1879. https://doi.org/10.1016/j.hazmat.2010.12.095.

Juhasz, A.L., Smith, E., Nelson, C., Thomas, D.J., Bradham, K., 2014a. Variability asso-ciated with As in vivo-in vitro correlations when using different bioaccessibility methodologies. Environ. Sci. Technol. 48, 11646–11653. https://doi.org/10.1021/ es502751z.

Juhasz, A.L., Herde, P., Herde, C., Boland, J., Smith, E., 2014b. Validation of the pre-dictive capabilities of the Sbrc-G in vitro assay for estimating arsenic relative bioa-vailability in contaminated soils. Environ. Sci. Technol. 48, 12962–12969. https:// doi.org/10.1021/es503695g.

Kastury, F., Smith, E., Karna, R.R., Scheckel, K.G., Juhasz, A.L., 2018. An inhalation-ingestion bioaccessibility assay (IIBA) for the assessment of exposure to metal(loid)s in PM$_{10}$. Sci. Total Environ. 631-632, 92–104. https://doi.org/10.1016/j.scitotenv. 2018.02.337.

Kim, K.H., Kabir, E., Kabir, S., 2015. A review on the human health impact of airborne particulate matter. Environ. Int. 74, 136–143. https://doi.org/10.1016/j.envint. 2014.10.005.

Kříbek, B., Majer, V., Knésl, I., Nyambe, I., Mihaljevič, M., Ettler, V., Sracek, O., 2014. Concentration of arsenic, copper, cobalt, lead and zinc in cassava (*Manihot esculenta* Crantz) growing on uncontaminated and contaminated soils of the Zambian

Copperbelt. J. Afr. Earth Sci. 99, 713–723. https://doi.org/10.1016/j.afrearsci.2014. 02.009.

Kříbek, B., Majer, V., Knésl, I., Keder, J., Mapani, B., Kamona, F., Mihaljevič, M., Ettler, V., Penížek, V., Vaněk, A., Sracek, O., 2016. Contamination of soil and grass in the Tsumeb smelter area, Namibia: modeling of contaminants dispersion and ground geochemical verification. Appl. Geochem. 64, 75–91. https://doi.org/10.1016/j. apgeochem.20015.07.006.

Kříbek, B., Šípková, A., Ettler, V., Mihaljevič, M., Majer, V., Knésl, I., Mapani, B., Penížek, V., Vaněk, A., Sracek, O., 2018. Variability of the copper isotopic composition in soil and grass affected by mining and smelting in Tsumeb, Namibia. Chem. Geol. 493, 121–135. https://doi.org/10.1016/j.chemgeo.2018.05.035.

Lábár, J.L., 2005. Consistent indexing of a (set of) SAED pattern(s) with the Process Diffraction program. Ultramicroscopy 103, 237–249. https://doi.org/10.1016/j. ultramic.2004.12.004.

Li, S.W., Sun, H.J., Li, H.B., Luo, J., Ma, L.Q., 2016. Assessment of cadmium bioaccessibility to predict its bioavailability in contaminated soils. Environ. Int. 94, 600–606. https://doi.org/10.1016/j.envint.2016.06.022.

Mapani, B., Ellmies, R., Kamona, F., Kříbek, B., Majer, V., Knésl, I., Pašava, J., Mufenda, M., Mbingeneeko, F., 2010. Potential human health risks associated with historic ore processing at Berg Aukas, Grootfontein area, Namibia. J. Afr. Earth Sci. 58, 634–647. https://doi.org/10.1016/j.afrearsci.2010.07.007.

Mapani, B., Uugulu, S., Hahn, R.L., Ellmies, R., Mwananawa, N., Amaambo, W., Schneider, G., 2011. Results of urine and blood from residents around the copper smelter complex, Tsumeb, Namibia: an example of anthropogenic contamination. In: Kříbek, B. (Ed.), Mining and the Environment in Africa, IGCP/SIDA Project 594 Inaugural Workshop, Kitwe, Zambia, pp. 48–50. Available from. http://geology.cz/igcp594.

Mapani, B., Ellmies, R., Hahn, L., Schneider, G., Ndalulilwa, K., Leonard, R., Zeeuw, M., Mwananawa, N., Uugulu, S., Namene, E., Amaambo, W., Sibanda, F., Mufenda, M., 2014. Contamination of agricultural products in the suuroundings of the Tsumeb smelter complex. In: Comm. Geol. Surv. Namibia 15. pp. 92–110. Available online. http://www.mme.gov.na/files/publications/381_Mapani%20et%20al_Contamination%20of%20Agricultural%20Products.pdf, Accessed date: 19 September 2018.

Martin, R., Dowling, K., Pearce, D., Sillitoe, J., Florentine, S., 2014. Health effects associated with inhalation of airborne arsenic arising from mining operations. Geosciences 4, 128–175. https://doi.org/10.3390/geosciences4030128.

Meunier, L., Walker, S.R., Wragg, J., Parsons, M.B., Koch, I., Jamieson, H.E., Reimer, K.J., 2010. Effects of soil composition and mineralogy on the bioaccessibility of arsenic from tailings and soil in gold mine districts of Nova Scotia. Environ. Sci. Technol. 44, 2667–2674. https://doi.org/10.1021/es9035682.

Mileusnic, M., Mapani, B.S., Kamona, A.F., Ružičic, S., Mapaure, I., Chimwamurombe, P.M., 2014. Assessment of agricultural soil contamination by potentially toxic metals dispersed from improperly disposed tailings, Kombat mine, Namibia. J. Geochem. Explor. 144, 409–420. https://doi.org/10.1016/j.gexplo.2014.01.009.

Molina, R.M., Schaider, L.A., Donaghey, T.C., Shine, J.P., Brain, J.D., 2013. Mineralogy affects geoavailability, bioaccessibility and bioavailability of zinc. Environ. Pollut. 182, 217–224. https://doi.org/10.1016/j.envpol.2013.07.013.

Morman, S.A., Plumlee, G.S., 2013. The role of airborne mineral dusts in human disease. Aeolian Res. 9, 203–212. https://doi.org/10.1016/j.aeolia.2012.12.001.

Morrison, A.L., Gulson, B.L., 2007. Preliminary findings of chemistry and bioaccessibility in base metal smelter slags. Sci. Total Environ. 382, 30–42. https://doi.org/10.1016/j.scitotenv.2007.03.034.

Morrison, A.L., Swierczek, Z., Gulson, B.L., 2016. Visualisation and quantification of heavy metal accessibility in smelter slags: the influence of morphology on availability. Environ. Pollut. 210, 271–281. https://doi.org/10.1016/j.envpol.2015.11.030.

Ojelede, M.E., Annegarn, H.J., Kneen, M.A., 2012. Evaluation of Aeolian emissions from gold mine tailings on the Witwatersrand. Aeolian Res. 3, 477–486. https://doi.org/10.1016/j.aeolia.2011.03.010.

Plumlee, G.S., Morman, S.A., 2011. Mine wastes and human health. Elements 7, 399–404. https://doi.org/10.2113/gselements.7.6.399.

Reis, A.P., Patinha, C., Noack, Y., Robert, S., Dias, A.C., Ferreira da Silva, E., 2014. Assessing the human health risk for aluminium, zinc and lead in outdoor dusts collected in recreational sites used by children at an industrial area of the western part of the Bassin Minier de Provence, France. J. Afr. Earth Sci. 99, 724–734. https://doi.org/10.1016/j.afrearsci.2013.08.001.

Romero, F.M., Villalobos, M., Aguirre, R., Gutiérrez, M.E., 2008. Solid-phase control on lead bioaccessibility in smelter-impacted soils. Arch. Environ. Contam. Toxicol. 55, 566–575. https://doi.org/10.1007/s00244-008-9152-3.

Skeaff, J.M., Thibault, Y., Hardy, D.J., 2011. A new method for the characterization and quantitative speciation of base metal smelter stack particulates. Environ. Monit. Assess. 177, 165–192. https://doi.org/10.1007/s10661-010-1627-9.

Sracek, O., Mihaljevič, M., Kříbek, B., Majer, V., Filip, J., Vaněk, A., Penížek, V., Ettler, V., Mapani, B., 2014a. Geochemistry of mine tailing and behaviour of arsenic at Kombat, northeastern Namibia. Environ. Monit. Assess. 186, 4891–4903. https://doi.org/10.1007/s10661-014-3746-1.

Sracek, O., Mihaljevič, M., Kříbek, B., Majer, V., Filip, J., Vaněk, A., Penížek, V., Ettler, V., Mapani, B., 2014b. Geochemistry and mineralogy of vanadium in mine tailing at Berg Aukas, northeastern Namibia. J. Afr. Earth Sci. 96, 180–189. https://doi.org/10.1016/j.afrearsci.2014.04.003.

Swartjes, F.A., Cornelis, C., 2011. Human health risk assessment. In: Swartjes, F.A. (Ed.), Dealing with Contaminated Sites. Springer Science + Business Media B.V, Berlin, pp. 209–259.

Thomas, A.N., Root, R.A., Lantz, R.C., Sáez, A.E., Chorover, J., 2018. Oxidative weathering decreases bioaccessibility of toxic metal(loid)s in PM$_{10}$ emissions from sulphide mine tailings. GeoHealth 2, 118–138. https://doi.org/10.1002/2017GH000118.

Tiesjema, B., Baars, A.J., 2009. Re-evaluation of some human-toxicological Maximum Permissible Risk levels earlier evaluated in the period 1991–2001. RIVM Report 711701092, Bilthoven, the Netherlands.

US EPA, 2007. Estimation of Relative Bioavailability of Lead in Soil and Soil-like Materials Using *in vivo* and *in vitro* Methods. 9285. Office of Solid Waste and Emergency Response, US EPA, Washington, OSWER, pp. 7–77.

Uzu, G., Sauvain, J.J., Baeza-Squiban, A., Riediker, M., Sánchez, M., Hohl, S., Val, S., Tack, K., Denys, S., Pradère, P., Dumat, C., 2011. In vitro assessment of the pulmonary toxicity and gastric availability of lead-rich particles from a lead recycling plant. Environ. Sci. Technol. 45, 7888–7895. https://doi.org/10.1021/es200374c.

Yabe, J., Nakayama, S.M.M., Ikenaka, Y., Yohannes, Y.B., Bortey-Sam, N., Orostlany, B., Muzandu, K., Choongo, K., Kabalo, A.N., Ntapisha, J., Mweene, A., Umemura, T., Ishizuka, M., 2015. Lead poisoning in children from townships in the vicinity of a lead-zinc mine in Kabwe, Zambia. Chemosphere 119, 941–947. https://doi.org/10.1016/j.chemosphere.2014.09.028.

Yabe, J., Nakayama, S.M.M., Ikenaka, Y., Yohannes, Y.B., Bortey-Sam, N., Kabalo, A.N., Ntapisha, J., Mizukawa, H., Umemura, T., Ishizuka, M., 2018. Lead and cadmium excretion in feces and urine of children from polluted townships near a lead-zinc mine in Kabwe, Zambia. Chemosphere 202, 48–55. https://doi.org/10.1016/j.chemosphere. 2018.03.079.

Zhao, D., Wang, J.Y., Tang, N., Yin, D.X., Luo, J., Xiang, P., Juhasz, A.L., Li, H.B., Ma, L.Q., 2018. Coupling bioavailability and stable isotope ratio to discern dietary and non-dietary contribution of metal exposure to residents in mining-impacted areas. Environ. Int. 120, 563–571. https://doi.org/10.1016/j.envin.2018.08.023.